Energy Storage

DOI: 10.1002/anie.201209259

Controlled Electrochemical Charge Injection to Maximize the Energy Density of Supercapacitors**

Zhe Weng, Feng Li, Da-Wei Wang, Lei Wen, and Hui-Ming Cheng**

To increase the energy density of supercapacitors (SCs), numerous attempts are focused on developing high-capacity electrode materials[1] and high-voltage electrolytes.[2] However, a common but very important problem that has not been solved is that the high specific capacity of electrode materials and the voltage window of electrolytes cannot always be fully used when assembled into SC devices. In early studies it was found that this problem results from the unsuitable electrode potential window (EPW) in SC devices.[3] In fact, both the working voltage and the specific capacity of SCs rely significantly on the EPW of individual electrodes. Therefore, the EPW must be optimized to maximize the energy density of SCs. Up to date, however, the unsuitable EPW can be moderated only by balancing the electrode mass[4] (as illustrated in Figure 1 a) or by using different materials as electrodes[3b,5] to assemble asymmetric SCs. The balancing of the electrode mass will increase the working voltage but not increase the specific capacity.[6] It is difficult and time consuming to find appropriate materials matching each other which can be used for the electrodes of an asymmetric SC. For Li-ion capacitors,[2a] prelithiating anodes can be used to enlarge the positive EPW for an increasing capacity,[7] but they are inapplicable to conventional SCs. Therefore, we consider that the adjustment of the electrode potential (EP) is the general key to optimizing the EPW.

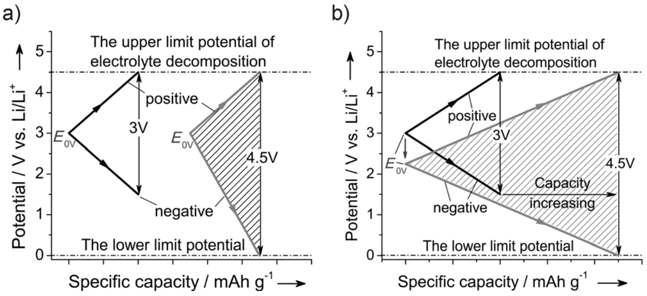

Figure 1. Positive and negative EP variation in a SC device during the charge process, illustrating two ways for improving the energy density. a) Increasing the mass of the positive electrode with a limited EPW to improve the working voltage, but the specific capacity will not increase. b) Optimizing the EPW by tuning E_{0V} to simultaneously increase the specific capacity and working voltage. The shadowed area is equal to the value of the energy density.

The EP depends on the surface charge density of the electrode materials for the SCs.[8] Therefore, it is feasible to tune the EP through changing the surface charge density. Electrochemical charge injection (ECI) as an available method for electrically inducing large changes in the charge density has been used to tune the bulk properties of materials, that is, the optical, electrical, and magnetic properties.[9] The mechanism of injecting charges into materials is the double-layer adsorption of counter ions or the Faradic reaction with counter ions through electrochemically charging the materials in electrolytes. Here, we demonstrate that controlled ECI can be used as an efficacious approach to tune the EP of electrode materials by controlling their surface chemical structure for optimizing their EPW. A series of SC devices based on various carbon materials, including graphene, carbon nanotubes, and porous carbon, were studied. Benefiting from this strategy, the energy density of the SCs can reach about 10 times the original values.

The carbon electrode materials used herein are chemically derived graphene,[10] multi-walled carbon nanotubes (MWCNTs), single-walled carbon nanotubes (SWCNTs), and hierarchical porous graphitic carbon (HPGC).[11] Their characterization is shown in Figure S1 and Table S1 in the Supporting Information. Conventional symmetric SCs based on these carbon materials were assembled using 1 M $LiPF_6$/ethylene carbonate (EC) + dimethyl carbonate (DMC) as electrolyte. The SCs based on chemically derived graphene will mainly be discussed below, and the performance of the other carbon SCs are shown in Figures S2–S4.

As reported by others using the same electrolyte,[12] our results show that the working voltage of all the symmetric SCs cannot be higher than 3 V, which is below the voltage window of the electrolyte (4.5 V). A metal Li wire was used as a quasi-reference electrode to monitor the EP variation during charge/discharge. As shown in Figure 2 a, the potential of both electrodes measured at zero voltage (E_{0V}) is about 3.5 V vs. Li/Li$^+$ for the graphene SC. When the SC is charged by 3 V, the negative EP decreases to 1.6 V vs. Li/Li$^+$, and the positive EP increases to 4.6 V vs. Li/Li$^+$, which is already above the upper potential limit of the electrolyte decomposition.

---

[*] Z. Weng, Prof. F. Li, Dr. L. Wen, Prof. H.-M. Cheng
Shenyang National Laboratory for Materials Science
Institute of Metal Research, Chinese Academy of Sciences
72 Wenhua Road, Shenyang 110016 (China)
E-mail: fli@imr.ac.cn
cheng@imr.ac.cn
Dr. D.-W. Wang
ARC Centre of Excellence for Functional Nanomaterials
Australian Institute for Bioengineering and Nanotechnology
The University of Queensland
St Lucia, Brisbane, QLD 4072 (Australia)

[**] This work was supported by the Ministry of Science and Technology of China (grant number 2011CB932604) and the National Science Foundation of China (grant numbers 50921004 and 51172239) and the Chinese Academy of Sciences.

Supporting information for this article is available on the WWW under http://dx.doi.org/10.1002/anie.201209259.

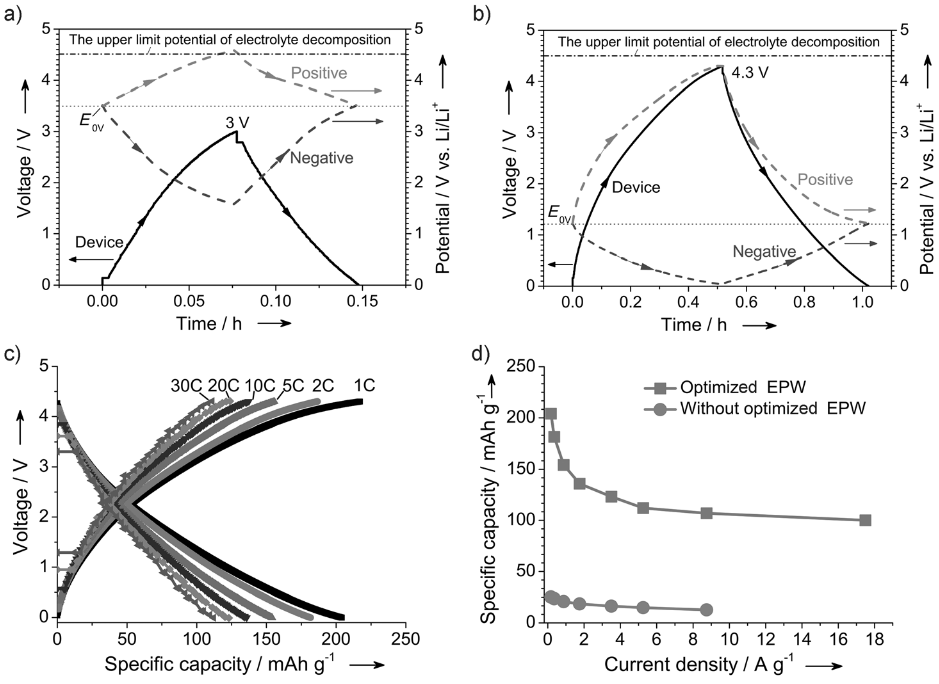

Figure 2. Charge/discharge profiles (at 0.35 $A g^{-1}$) of a) a conventional symmetric graphene SC and b) a graphene SC with optimized EPW by shifting E_{0V} down to 1.16 V vs. Li/Li$^+$. c) Charge/discharge curves of the graphene SC with optimized EPW at different current densities (1 C = 175 $mA g^{-1}$). d) Comparison of the specific capacity of graphene in the SCs with and without optimized EPW.

Clearly, the working voltage is limited by the positive electrode, which is due to the excessively high E_{0V}. If the E_{0V} can be tuned downwards to widen the positive EPW and shift the negative EPW downwards, the working voltage can be extended to be as wide as the entire voltage window of the electrolyte, and the specific capacity can be increased because of the extended EPW of the electrodes, as illustrated in Figure 1b. Both synergistically results in a much higher energy density.

The charges stored at positive and negative electrodes are equivalent:[6] $q = Q_+m_+ = Q_-m_-$, where Q_+ and Q_- are the specific capacities of positive and negative electrodes, and m_+ and m_- are the masses of active material on each electrode. Consequently, the specific capacity of a SC device can be expressed as given in Equation (1).

$$Q = \frac{q}{m_+ + m_-} = \frac{Q_+Q_-}{Q_+ + Q_-} \tag{1}$$

It is obvious that the maximum specific capacity of the SC is achieved only when $Q_+ = Q_-$ and $m_+ = m_-$. According to the energy density of SCs:[1a] $E = 1/2QU$, where U is the working voltage; a SC will reach its maximum energy density, when its two electrodes have the same specific capacity and its working voltage is the whole voltage window of the electrolyte used. As discussed, Q_+ and Q_- are dependent on the positive and negative EPW. Therefore, we can adjust E_{0V} to make $Q_+ = Q_-$ and enlarge the working voltage to the whole voltage window of the electrolyte. The way to determine the optimum E_{0V} is shown in the Supporting Information. The experimental results show that when E_{0V} is 1.16 V vs. Li/Li$^+$, $Q_+ = Q_-$ in the graphene SC (Figure S5). This result indicates that 1.16 V vs. Li/Li$^+$ is the optimum E_{0V} for the graphene SC, and its energy density will be maximized after tuning E_{0V} to this value. It is noteworthy that the optimum E_{0V} should differ for different electrode materials, and probably even for the same material in different electrolytes. As shown in Figures S2–S4b, the other carbon materials do show different E_{0V}. These results further indicate that the surface chemistry and microstructure of electrode materials, such as surface functional groups, surface area and defects, and electrolytes are critical for the EP tuning.

Taking graphene immersed in a lithium-ion electrolyte as an example, the variation of the surface chemical structure and EP with the amount of injected charge is shown in Figure 3. As injected electrons increase, the surface density of lithium ions absorbed on graphene by the electric double layer increases, and hence the EP shifts downwards. In addition to the non-faradic charge injection, as the surface charge density further increases, a surface redox reaction of lithium ions with graphene can take place. When EP shifts to about 1.5 V vs. Li/Li$^+$, the surface oxygen functional groups at the edge of graphene, such as carbonyl (>C=O) or carboxyl (O−C=O), begin to be reduced to C-O-Li.[13] Between 1.0 and 0.5 V vs. Li/Li$^+$, the faradic adsorption of lithium ions happens at the edges and defects of graphene.[14] Below 0.5 V vs. Li/Li$^+$, lithium ions can be adsorbed onto the geometric center of benzene rings.[12a] Therefore, the

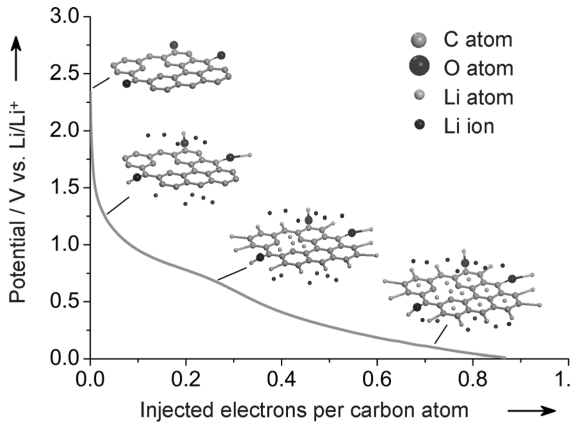

Figure 3. Variation of the surface chemical structure and the EP with the amount of injected charge (per carbon atom) for a graphene electrode in 1 M $LiPF_6$/EC + DMC electrolyte.

different EP corresponds to the different surface chemical structure of electrode materials.

In order to tune the EP, the ECI was adopted to control the surface chemical structure of carbon materials. Two identical graphene electrodes were separately assembled into two half-cells. The positive one was discharged to 1.16 V and then held at this voltage for 2 h to ensure the stabilization of the injected charge in the electrode. The negative one was first carried out with galvanostatic charge/discharge cycles in the voltage range of 0.01–1.16 V until a stable solid-electrolyte interphase film was built on graphene and then held at 1.16 V for 2 h. After injecting the charge, the potential of both electrodes was shifted to 1.16 V vs. Li/Li$^+$ because of the formation of the corresponding surface chemical structure. The EP of the other carbon materials was adjusted using the same process. Finally, the two electrodes with tuning EP were disassembled from the half-cells and assembled into a SC device.

The SCs with the tuned $E_{0\mathrm{V}}$ were tested by galvanostatic charge/discharge under 4.3 V instead of 4.5 V to avoid the electrolyte decomposition at high current densities. The potential profiles of the graphene SC are shown in Figure 2b and c, and the other carbon SCs are shown in Figures S2–S4. As expected, even under the high working voltage, all the SCs can work very well at different current densities, and each electrode operates in its optimum designed EPW. More importantly, the specific capacity of the carbon materials in all the SCs also remarkably increases because of the optimized EPW (Figure 2d and Figures S2–S4d). In a conventional SC, the capacity is only contributed by the double layer absorption of Li$^+$ or PF_4^- ions. After optimizing the EPW, however, the additional faradic reactions mentioned before happen on electrodes, which provide a large amount of faradic capacity. Therefore, both the voltage window of the electrolytes and the capacity of the active materials can be fully used after optimizing the EPW.

Due to the simultaneous widening of the working voltage and improvement of the specific capacity, the energy density of the carbon SCs can reach about ten times the original values, while a high power density is maintained at the same time, as shown in the Ragone plot (Figure 4). It is obvious that, after optimizing the EPW, the carbon SCs can store a higher energy relative to the best values reported for SCs and the value of Ni-MH batteries. The graphene SC can even provide more energy than lithium-ion batteries at a high-power output. Note that the carbon materials are used just as diverse examples which have not been optimized yet; thus further optimization of the electrode materials probably will give rise to an improved performance. Moreover, it has been proven that the SCs with optimized EPW have a long cyclic life (Figure S6).

In summary, we demonstrate that tuning the EP by controlled ECI to optimize the EPW is an efficacious strategy for maximizing the energy density of SC devices. A series of ultrahigh-energy carbon SCs were investigated by using this strategy. Benefiting from the simultaneous achievement of the maximum working voltage and specific capacity, the energy density of all the SCs studied has been increased about tenfold to a level close to that of lithium-ion batteries but without loss in power delivery and cyclic stability. We believe that our strategy is general and should be applicable to SCs based on other aqueous or non-aqueous electrolytes and other electrode materials, such as metal oxides and conducting polymers.

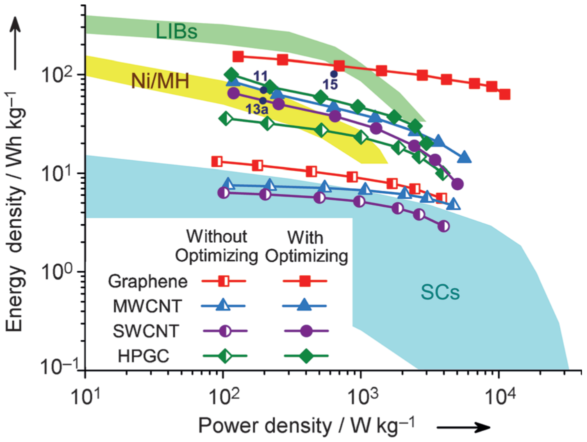

Figure 4. Ragone plot of our carbon SCs with and without optimized EPW (based on the total mass of the active material). The dots with the number of the appropriate references represent the best reported performances of the SCs based on graphene,[15] MWCNTs,[13a] and HPGC[11]. The performance of conventional SCs, lithium-ion batteries (LIBs) and Ni/MH batteries is estimated from the values in the Ragone plot of a previous review paper[1b] by multiplying a factor of 3, because the weight of the active material usually accounts for about 30% of the total mass of the packaged devices.[16]

Received: November 19, 2012

Keywords: carbon nanotubes · energy storage · graphene · supercapacitors

---

[1] a) G. P. Wang, L. Zhang, J. J. Zhang, *Chem. Soc. Rev.* **2012**, *41*, 797–828; b) P. Simon, Y. Gogotsi, *Nat. Mater.* **2008**, *7*, 845–854; c) R. Liu, J. Duay, S. B. Lee, *Chem. Commun.* **2011**, *47*, 1384–1404; d) J. T. Zhang, X. S. Zhao, *ChemSusChem* **2012**, *5*, 818–841.

[2] a) K. Naoi, *Fuel Cells* **2010**, *10*, 825–833; b) P. J. Hall, M. Mirzaeian, S. I. Fletcher, F. B. Sillars, A. J. R. Rennie, G. O. Shitta-Bey, G. Wilson, A. Cruden, R. Carter, *Energy Environ. Sci.* **2010**, *3*, 1238–1251; c) A. Brandt, A. Balducci, *J. Electrochem. Soc.* **2012**, *159*, A2053–A2059.

[3] a) M. P. Bichat, E. Raymundo-Pinero, F. Beguin, *Carbon* **2010**, *48*, 4351–4361; b) V. Khomenko, E. Frackowiak, F. Beguin, *Electrochim. Acta* **2005**, *50*, 2499–2506; c) D. Qu, *J. Appl. Electrochem.* **2009**, *39*, 867–871.

[4] L. Demarconnay, E. Raymundo-Pinero, F. Beguin, *J. Power Sources* **2011**, *196*, 580–586.

[5] V. Khomenko, E. Raymundo-Pinero, F. Beguin, *J. Power Sources* **2010**, *195*, 4234–4241.

[6] C. Peng, S. W. Zhang, X. H. Zhou, G. Z. Chen, *Energy Environ. Sci.* **2010**, *3*, 1499–1502.

[7] a) T. Aida, K. Yamada, M. Morita, *Electrochem. Solid-State Lett.* **2006**, *9*, A534–A536; b) V. Khomenko, E. Raymundo-Pinero, F. Beguin, *J. Power Sources* **2008**, *177*, 643–651.

[8] B. E. Conway, *Electrochemical Supercapacitors: Scientific Fundamentals and Technological Applications*, Kluwer Academic/Plenum Publisher, New York, **1999**.

[9] A. A. Zakhidov, D. S. Suh, A. A. Kuznetsov, J. N. Barisci, E. Munoz, A. B. Dalton, S. Collins, V. H. Ebron, M. Zhang, J. P. Ferraris, R. H. Baughman, *Adv. Funct. Mater.* **2009**, *19*, 2266–2272.

[10] Z. Weng, Y. Su, D. W. Wang, F. Li, J. H. Du, H. M. Cheng, *Adv. Energy Mater.* **2011**, *1*, 917–922.

[11] D. W. Wang, F. Li, M. Liu, G. Q. Lu, H. M. Cheng, *Angew. Chem.* **2008**, *120*, 379–382; *Angew. Chem. Int. Ed.* **2008**, *47*, 373–376.

[12] a) B. Z. Jang, C. G. Liu, D. Neff, Z. N. Yu, M. C. Wang, W. Xiong, A. Zhamu, *Nano Lett.* **2011**, *11*, 3785–3791; b) M. D. Stoller, S. Murali, N. Quarles, Y. W. Zhu, J. R. Potts, X. J. Zhu, H. W. Ha, R. S. Ruoff, *Phys. Chem. Chem. Phys.* **2012**, *14*, 3388–3391.

[13] a) S. W. Lee, N. Yabuuchi, B. M. Gallant, S. Chen, B. S. Kim, P. T. Hammond, Y. Shao-Horn, *Nat. Nanotechnol.* **2010**, *5*, 531–537; b) X. Y. Han, G. Y. Qing, J. T. Sun, T. L. Sun, *Angew. Chem.* **2012**, *124*, 5237–5241; *Angew. Chem. Int. Ed.* **2012**, *51*, 5147–5151.

[14] D. Y. Pan, S. Wang, B. Zhao, M. H. Wu, H. J. Zhang, Y. Wang, Z. Jiao, *Chem. Mater.* **2009**, *21*, 3136–3142.

[15] C. G. Liu, Z. N. Yu, D. Neff, A. Zhamu, B. Z. Jang, *Nano Lett.* **2010**, *10*, 4863–4868.

[16] Y. Gogotsi, P. Simon, *Science* **2011**, *334*, 917–918.